A Simplified Analytical Method for Wound Pressure Vessel Design

Author

MUHAMMAD ADNAN KHAN

Regn Number

00000205648

Supervisor

Dr. Hasan Aftab Saeed

DEPARTMENT MECHANICAL ENGINEERING

SCHOOL OF MECHANICAL & MANUFACTURING ENGINEERING

NATIONAL UNIVERSITY OF SCIENCES AND TECHNOLOGY

ISLAMABAD

DECEMBER, 2020

A Simplified Analytical Method for Wound Pressure Vessel Design

Author

MUHAMMAD ADNAN KHAN

Regn Number

00000205648

A thesis submitted in partial fulfillment of the requirements for the degree of

MS Mechanical Engineering

Thesis Supervisor:

Dr Hasan Aftab Saeed

Thesis Supervisor's Signature: _____

DEPARTMENT MECHANICAL ENGINEERING

SCHOOL OF MECHANICAL & MANUFACTURING ENGINEERING

NATIONAL UNIVERSITY OF SCIENCES AND TECHNOLOGY,

ISLAMABAD

DECEMBER, 2020

Declaration

I certify that this research work titled "A simplified analytical method for wound pressure vessel design*"* is my own work. The work has not been presented elsewhere for assessment. The material that has been used from other sources it has been properly acknowledged / referred.

Signature of Student

MUAHMMAD ADNAN KHAN

00000205648

Language Correctness Certificate

This thesis has been read by an English expert and is free of typing, syntax, semantic, grammatical and spelling mistakes. Thesis is also according to the format given by the university.

Signature of Student

Muhammad Adnan Khan

Registration Number

00000205648

Signature of Supervisor

Plagiarism Certificate (Turnitin Report)

This thesis has been checked for Plagiarism. Turnitin report endorsed by Supervisor is attached.

Signature of Student

Muhammad Adnan Khan

Registration Number

00000205648

Signature of Supervisor

Copyright Statement

- Copyright in text of this thesis rests with the student author. Copies (by any process) either in full, or of extracts, may be made only in accordance with instructions given by the author and lodged in the Library of NUST School of Mechanical & Manufacturing Engineering (SMME). Details may be obtained by the Librarian. This page must form part of any such copies made. Further copies (by any process) may not be made without the permission (in writing) of the author.
- The ownership of any intellectual property rights which may be described in this thesis is vested in NUST School of Mechanical & Manufacturing Engineering, subject to any prior agreement to the contrary, and may not be made available for use by third parties without the written permission of the SMME, which will prescribe the terms and conditions of any such agreement.
- Further information on the conditions under which disclosures and exploitation may take place is available from the Library of NUST School of Mechanical & Manufacturing Engineering, Islamabad.

Acknowledgements

I am thankful to my Creator Allah Subhana-Watala to have guided me throughout this work at every step and for every new thought which You setup in my mind to improve it. Indeed, I could have done nothing without Your priceless help and guidance. Whosoever helped me throughout the course of my thesis, whether my parents or any other individual was Your will, so indeed none be worthy of praise but You.

I am profusely thankful to my beloved parents who raised me when I was not capable of walking and continued to support me throughout in every department of my life.

I would also like to express special thanks to my supervisor DR. Hasan Aftab Saeed for his help throughout my thesis and also for Mechanical APDL and Finite Element Method courses which he has taught me. I can safely say that I haven't learned any other engineering subject in such depth than the ones which he has taught.

I would also like to pay special thanks to Dr. Hasan Aftab Saeed for his tremendous support and cooperation. Each time I got stuck in something, he came up with the solution. Without his help I wouldn’t have been able to complete my thesis. I appreciate his patience and guidance throughout the whole thesis.

I would also like to thank Dr. Sajid Ullah Butt and Dr. Naveed Akmal Din for being on my thesis guidance and evaluation committee and express my special thanks for their support and cooperation.

Finally, I would like to express my gratitude to all the individuals who have rendered valuable assistance to my study

Dedicated to my exceptional parents and adored siblings whose tremendous support and cooperation led me to this wonderful accomplishment.

Nomenclature

θ_a is the starting helix angle at smaller radius (r)

θ_b is the starting helix angle at Larger radius (R)

t_R is the thickness of fiber tape at winding angle (θ)

m_R is the qquantity of the fibers tapes to make a layer

n_R is the number of the single plies

t_p is the fiber thickness

r_o is the radius of dome at the pole position

b is the fiber width

m_o is quantity of fiber tapes at the pole of the dome

n_o is quantity of single plies at the pole of the dome

t_R is thickness of the laminates in the cylindrical section of the vessel

V_{cons} is the constant

L_v is the total length of the vessel

D_v is cylindrical diameter

L_d is the length of the dome

D_p is the diameter of the dome

Abstract

Composite materials are used to manufacture pressure vessel due to their light weight and higher physical properties. Continuous filament winding process is used to make composite pressure vessels (CPVs) in which fiber is wound over a mandrel. Resultantly, complex interlaced winding pattern especially in the dome section which could significantly affect mechanical behavior and vessel under the internal pressure composite pressure vessel because the layup sequence flips from mosaic to mosaic. This work focuses on analytical approach for finding out the fiber thickness which requires more attention for the optimum design and analysis of CPVs constructed by continuous filament winding process. This new analytical method is obtained by approximating the surface of complete vessel and validated with cubic spline function and Gramoll and Namiki methods [1]. The results have been validated and are quite promising with regards to better accuracy and safety.

Key Words: *Fiber thickness, Dome thickness, kinematic constraints, composite pressure vessels*

Table of Contents

List of Figures

List of Tables

CHAPTER 1

1. INTRODUCTION

1.1. Motivation

Composite pressure vessels (CPVs) have several researches, industrial and defense applications because of their efficiency and stability in the harsh environments. They offer a significant reduction in weight when compared with conventional pressure vessels made up of either Steel or Aluminum. Continuous filament winding technique is being used for the manufacturing of the composite pressure vessels in which fiber tape is wound over the mandrel at specific helix angle which totally depends upon the profile of the dome [2]. Fiber is wound on the mandrel in such a way that there must be maximum friction between the fiber tapes and the path of this minimum slipping condition is known as geodesic path as shown in the figure 1.

Figure 1.1: Aluminum liner for a composite pressure vessel. [3]

As profile of cylindrical portion remains constant, so helix angle does not change throughout this section but helical angle changes in the dome as a result of changing profile of this section. Moreover, fiber passes tangent to the pole of vessel but perpendicular to the meridian of the vessel which indicates that fiber has to make more overlapping in the dome portion which is responsible for the increment of fiber thickness in this section. Cubic spline function has been

developed for the calculation of the dome thickness in which four coefficients are required to find out which totally depends upon the helical angle and profile of the dome portion. Dome thickness calculated by different method is given below.

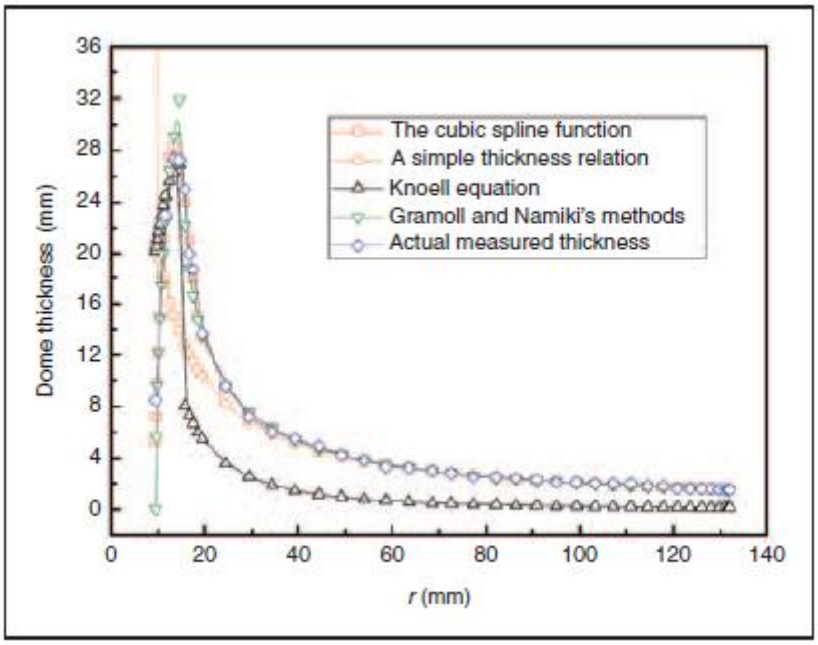

Figure 1.2 Thickness of fiber in Dome forecasted by different methods [1].

Similarly, Gramoll and Namiki methods are the relatively complex methods to calculate the dome thickness. Previous analysis involves the prediction of fiber thickness in the dome of vessel using Cubic Spline Function and Finite Element Analysis (FEA) but this analysis involves a new analytical method to prediction the dome thickness which gives the optimum design of the vessel. This paper deals with the analytical approach to find out the fiber thickness in dome of vessel and compare this new mathematical approach with cubic spline function and Gramoll and Namiki methods. Profile of pressure vessel is selected from the [1]. Differences in the results could be understood that method described in this research work has less relative error as compare to above mentioned methods and moreover, the approximated method is a simple and easy method. Filament winding process is a continuous process in which fiber starts in such a way that it must passes tangent to the opening of the pole and perpendicular to the meridian of the mandrel. As filament winding is a continuous process in which fiber wound from pole of 1st dome and moves towards the pole of 2nd dome and then moves towards the pole of 1st dome, so there are two angles 1st is positive angle and other is

negative angle. These angles have same magnitude but different directions. Helical angle totally depends upon the geometry of the dome. As geometry of the dome has not a constant profile, so helical angle varies from pole to the equator of the vessel which remains constant throughout the cylindrical portion due to constant profile. Overlapping of fiber tapes occurs from equator to the pole due to change in the helical angle. As it has been stated that, structures made up of the composite fiber have relatively high strength and very low stiffness as compared to conventional metals.

1.2. Problem Statement

Composite pressure vessel (CPV) is made from winding continuous fibers over a mandrel. Resultantly, complex inter-laced winding pattern evolved [4]. Analytical modeling and FEA analysis, which require helical angle and actual fiber thickness as inputs for analysis, which can be actually find out by different methods. Analytical formulation for the calculation of the helical angle is well known as Clairant equation. Cubic spline function has been developed for the calculation of the dome thickness in which four coefficients are required to find out which totally depends upon the helical angle and profile of the dome portion. Similarly, Gramoll and Namiki methods are the relatively complex methods to calculate thickness of the fiber in the dome.

1.3. Aim and Objective

The core intention of this study thesis is to find the analytical method to find out the fiber thickness in the dome for optimum design of pressure vessel. The following secondary goals were taken to achieve the above-mentioned primary goal.

1. Overlapping of fiber in anywhere of pressure vessel at helix angle.
2. To develop MATLB code for finding helical winding at helix angle.
3. To developed MATLAB code for finding out the gap between starting and ending point of fiber at helical angle.
4. Overlapping of fiber tape within the dome profile.
5. Find the thickness of fiber in dome of vessel.
6. Compare the results of fiber thickness with methods mentioned in the research work name [1].

1.4.Outlines of thesis

This research thesis is general solution for finding out the fiber thickness in dome of vessel for the optimum design of composite pressure vessel. This research work consists of seven stages. In 1st stage, MATLAB code is developed that gives helical winding at helix angle. In the 2nd stage, MATLAB is developed that gives the gap between starting and ending point of fiber tape in the vessel. In the 3rd stage, analytical approach is developed for finding out the overlapping of the fiber tapes. In the 4th stage, developing a new analytical approach for finding the fiber thickness in the dome has been performed. Comparison of this analytical approach with the Cubic Spline Function and Gramoll and Namiki methods [1] in the 5th stage.

CHAPTER 2

2. LITERATURE REVIEW

Modern industry is looking to improve quality of its product for better performance that requires huge improvement of structural materials. Composite materials are the promising kind of engineering materials [5]. These engineered materials are getting attention due to their better properties like stiffness, strength and high structural properties that facilitate them to be applied in a vast variety of fields, particularly, the application of vessels made up of composite materials have increased to astronomical, gas carrying cylinder like LPG or CNG gas carrying cylinders. Generally, design thoughts used in aerospace field must be varied for marketable pressure vessels in order to fabricate for better dependability and affordable mass. A wound composite pressure vessel can be idealized in figure 2.1.

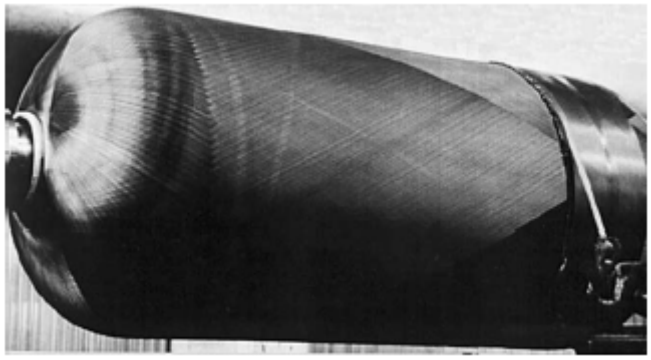

Figure 2.1: These engineered materials are getting attention [6]

The continuous filament winding technique is being used for the fabrication of the spinning shapes, particularly for the pressure tanks [2]. Structural behavior of filament-wound composites is characterized by different parameters which are ultimately a function of primary process parameters. Selection of proper material which is suitable for the working environment is the key parameter which makes pressure vessel in better performance. Secondly manufacturing factors in which angle on geodesic path, proper fiber thickness with suitable stacking sequence and selection of fiber bandwidth are the main factors upon which dependency of manufacturing processes lie. Consequently, it's very important to urge command on filament winding process factors for orthotropic and layered construction exploitation [7]. Designing, development and structural investigation of superior pressure

vessels are generally established on the mechanics of composite laminates [3] with respect to the fiber orientation, fiber thickness and no of plies. Cross sectional area of the dome thickness is being shown in the figure 2.2, in which dome thickness is clearly seen. Dome thickness is smaller at equator and then increases towards pole and become equal to the sum of fiber tows used to fill the mandrel for helical session.

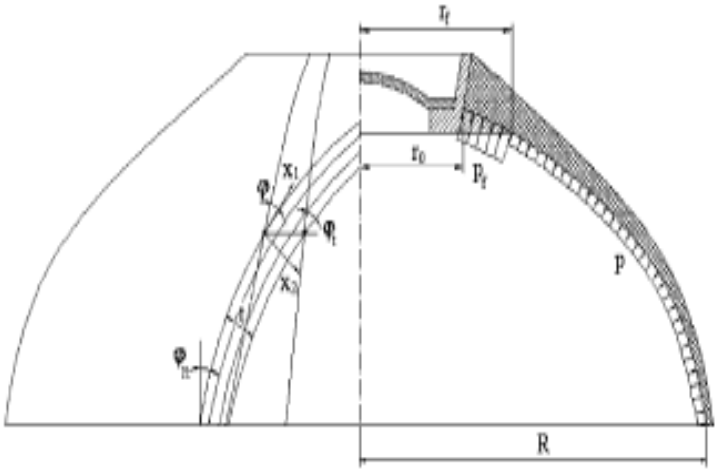

Figure 2.2: Cross sectional area of Dome of the vessel [6].

Overlapping of fiber tapes from cylindrical portion to the pole of vessel become more as shown in the figure 2.2. Moreover, number of the tapes winding over the cylindrical portion remains constants throughout the vessel which make fiber thicker on the pole of vessel. As discussed earlier that vessel made up of filament winding process in which fiber tape wound over the mandrel resultantly, complex inter-laced winding pattern evolved which needs to be considered for optimum design of the vessel. A simple laminated structure comprises of different layers with different fiber orientation, but a continuous filament wound vessel has two plies with same helical angle but in opposite direction i.e $+\theta$ and $-\theta$ in each helical session [8] as shown in the figure 2.4.

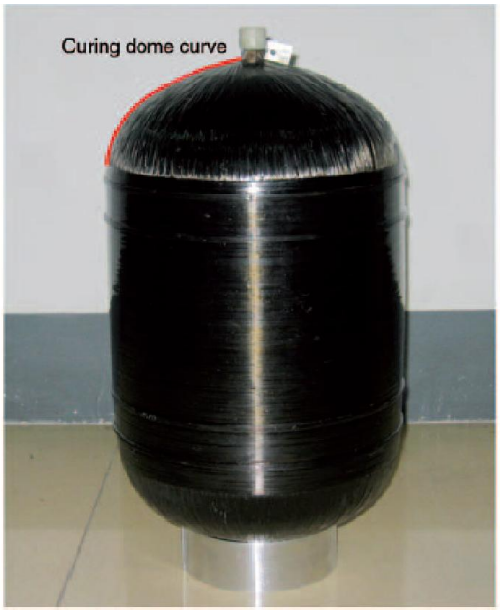

Figure 2.3: Filament wound pressure vessel [1]

Composite pressure vessel made up of continuous filament winding process has two regions: major crossovers in which fibers are overlapped and minor crossovers in which helical angle suddenly varies [7] as shown in the figure 2.4. Figure 2.4 shows that fiber there are two angles in one helical session which have same magnitude but have different direction. One angle is positive and other is negative angle. Moreover, in the major crossover region, when a fiber with negative angle passes over the fiver wound with negative angle gets overlapped which is responsible for the increasing of the dome thickness.

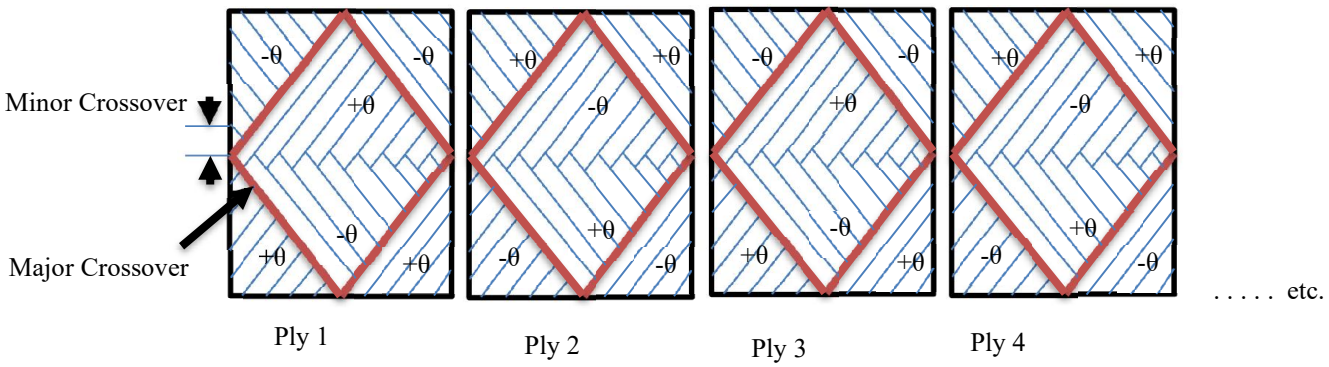

Figure 2.4: stacking sequence of fiver in laminate wound composite [4]

These regions bond to form mosaic shapes or three-sided iterating mosaic shapes with interchanging $\pm\theta$ and $\mp\theta$ alignments as shown in the figure 2.5. These alternating patterns are responsible for elastic coupling among the structure, and additionally, influence its structural behavior that causes the laminates to perform in an unusual way [8]. Moreover, these helical wound layers are added on the cylindrical portion of the cylinder, the curving path of dome portion is responsible for continuous change within the fiber thickness and fiber is thicker closer to the pole [9].

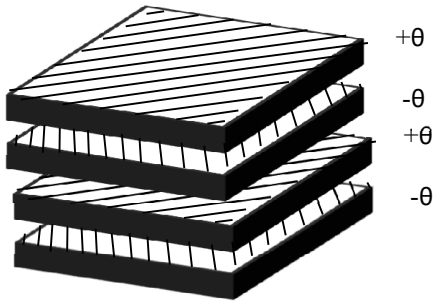

Figure 2.5: Fiber Layers with ±θ and ± θ Orientation

Continuous filament winding process is a continuous technique of manufacturing composite pressure vessels with fiber must be perpendicular to the meridian of the vessel and passes tangent to the pole of the dome. Fiber follows a path involving minimum slipping condition, this path is called as geodesic path which depends upon the surface over which fibers are wound (Figure 2.6). Figure 2.6 shows 3D views of pressure vessels. Right hand ride vessel is drawn in the 3D generating software and left-hand side vessel is actual vessel. These vessels are labelled with different parts. Pole is the opening of the vessel at the end of the dome, Meridians are the line passing equivalent to the horizontal alignment of the vessel. Equator is point of leaving cylindrical portion and entrance of the dome. When fiber is bound to be wound on the geodesic path then fiber has to pass tangent to the pole of dome as shown in the figure 2.6.

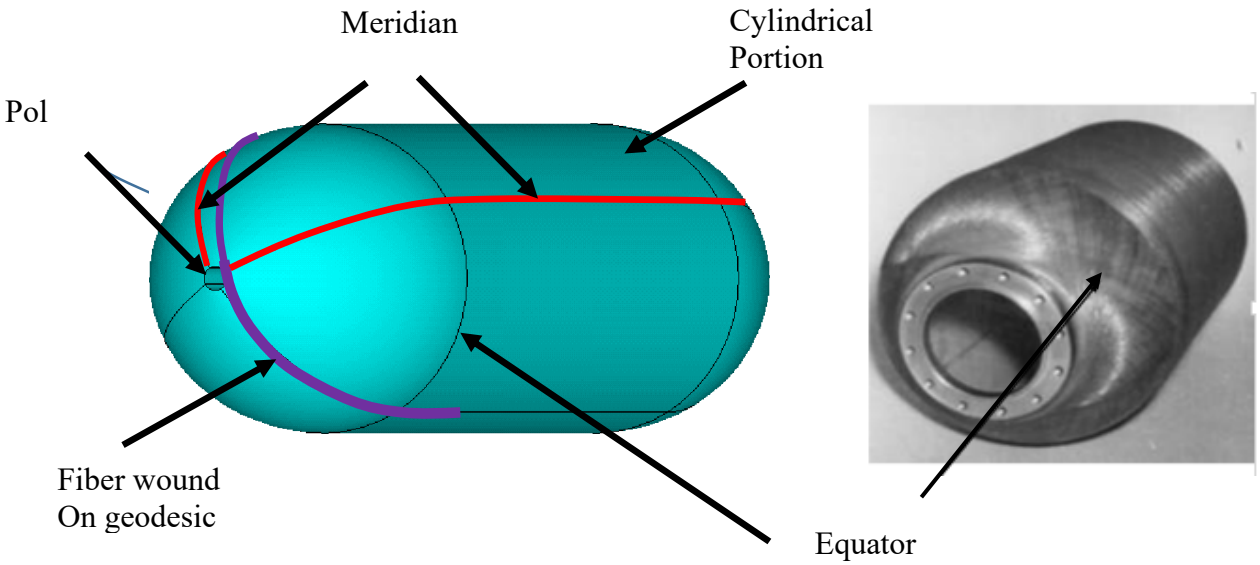

Figure 2.6: CAD model and actual composite vessel showing the geodesic path.

2.1. Winding based on geodesic path

Continuous filament winding technique is being used for the manufacturing of the composite pressure vessels in which fiber tape is wound over the mandrel at specific helix angle which totally depends upon the profile of the dome [10]. Fiber is wound on the mandrel in such a way that there must be maximum friction between the fiber tapes and the path of this minimum slipping condition is known as geodesic path. As profile of cylindrical portion remains constant, so helix angle does not change throughout this section but helical angle changes in the dome as a result of changing profile of this section. Moreover, fiber passes tangent to the pole of vessel but perpendicular to the meridian of the vessel which indicates that fiber has to make more overlapping in the dome portion which is responsible for the increment of fiber thickness in this section.

Resultantly, winding angle varies in the thickness direction as this angle depends upon the surface on that fibers are wound [5]. Helix angle is given below

$$\theta_b = \mathrm{Sin}^{-1}\left(\frac{r \sin(\theta_a)}{R}\right) \quad (2.1)$$

θ_a is the starting helix angle at smaller radius (r) of the dome and θ_b is the ending angle at the larger radius (R) of the dome. This is well known as Clairant equation [11]. MATLAB code is developed to get winding at any helical angle and this code is given in the Annex A.

2.2. Overlapping of fiber tapes

The process of making wound pressure vessels with openings on both sides in which each fiber tape cross over each other in a proper way and each tape should be tangent to the opening of vessel at pole radius. As number of fiber tapes crossing over the cylindrical portion remains same throughout the vessel because of the continuity [4]. This situation indicates that fiber tapes get more overlapped from the cylindrical portion to the pole of the vessel. Infect all the tapes pass at a same point of the pole which means that fiber tapes are 100% over lapped at this portion as shown in the figure 2.7. On the other hand, increment of the helical angle from equator to the pole of the vessel makes the fibers overlapped each other that is responsible for the increment of the dome thickness.

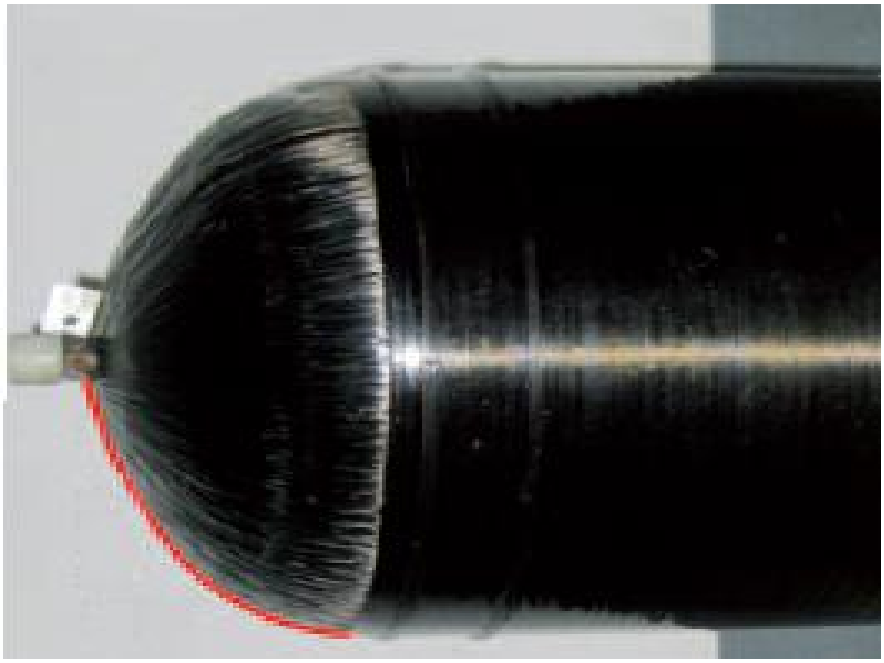

Figure 2.7: Overlapping of the fiber tap

2.3. Dome thickness

As dome of the vessels has varying profile which makes it complex for estimation of the dome thickness [8]. A basic relationship for calculation of the dome thickness in the dome portion is given below.

$$t(r) = \frac{R \cos \theta_o}{r \cos \theta} \text{x } t_R \tag{2.2}$$

Whereas t_R is the thickness of fiber tape at winding angle (θ) in the dome at (r) radius and (θ_o) is the helical angle in the cylindrical portion at (R) radius of the vessel. Above equation is based on the assumption that fiber tape is infinitely thin it means that this relation ignores the fiber tape width. Overlapping is directly proportion to the fiber width and due to which the dome thickness is directly proportion the overlapping of the tapes. A lot of research works have been presented for furcating of the thickness of the curvilinear portion of the vessels. Application of this work is limited for the pressure vessel used at the small scale because of the restriction of cartography. Equation (1) is developed with the assumption that band of the fiber is always infinitely thin, but when this equation is used to find out the thickness at the pole, it become clear that dome thickness is supposed to be considerably thin at the pole of the vessel. For this purpose, a lot of research works have been performed. An empirical method has been presented by Steng researcher which gives the number of plies at any required position. This method has limitations due to the complexity. After that Knoell proceeded his own research that gives a series of analytical equations for prediction the thickness. He adopted Stang concept but in different way. Similarly, Gramoll and Namiki (7) worked to give the solution of finding the dome thickness by giving two refined equations, predominantly at the point nearer to the pole of the dome where the fiber actually get 100% overlapped. This works tells that dome thickness is zero at the pole radius which actually does not exist. Cubic spline function was developed to forecast the thickness of laminates in the dome portion. This technique is based on the finding out the angle between band width in the dome which does not involve the actual profile of the dome portion.

In this research article, a simplified analytical method is presented to guess the fiber thickness. Adopting this simplified analytical method, a simplified analytical solution is presented which gives the thickness of fiber in the curvilinear portion of the vessels After that, precision of this novel analytical method is compared for estimation of the thickness in dome of composite pressure vessels at different points with the published research [1].

CHAPTER 3

3. Cubic spline Function

Making wound pressure vessels is a continuous filament winding process in which each fiber tape cross over each other in such a way that each fiber tape cross tangentially to the pole radius. Tapes of the fiber tapes are wound over the profile of the mandrel at the path of maximum friction and joint side by side to make a layer [12]. Profile of the dome and winding mosaic patterns are the fundamental factors for the making of the composite pressure vessel. Figure 3.1 shows the side view of a dome with almost one helical circuit. Figure 3.1 shows that location of the fiber tapes with their locations and development of the mandrel is given. It is supposed that fiber tapes are straight, which are actually in the curvilinear shape from equator to the pole of the vessels. This assumption is made for the finding out the thickness in the dome of the vessel because of the reason that the thickness becomes thin near the pole. If the number of the fiber tapes at anywhere of the dome radius is derived then the thickness knows how to be easily calculated.

3.1. Dome thickness within one-band width

Tapes of fiber are located in such a way that they are bounded side-to-side to make a layer. Quantity of the fibers tapes to make a layer is represented by m_R and the number of the single plies ($\pm\alpha_o$) is represented by n_R at the cylinder section. Hence the total number fiber m_R x n_R [1].

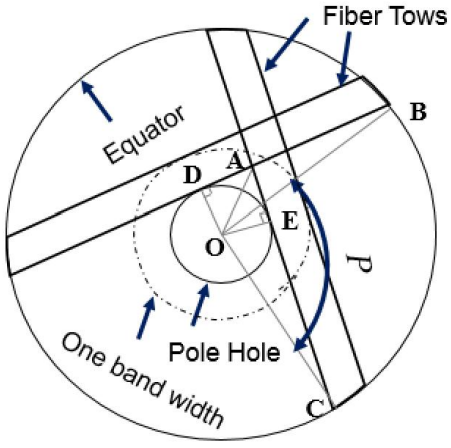

Figure 3.1: Pictorial correlation about fiber bands in one band width

As winding process is a continuous filament winding process in which number of the fiber tapes remains constant due to its continuity. Which is equal to the number of fiber tapes passing in the cylindrical portion.

$$t(r) = \frac{p}{2\pi}.m_R.n_R.t_p \ (r_o \leq r \leq r_o + b) \tag{3.1}$$

Where p is ∠BOC, t_p the fiber thickness which is constant though out the vessel; r_o the radius of dome at the pole position; b the fiber width and r an arbitrary shell radius within one-band width.

$$p = \angle BOC = \angle BOE + \angle COE = \angle COE + (\angle AOD + \angle AOE - \angle BOD)$$

$$p = Cos^{-1}\left(\frac{ro}{R}\right) + Cos^{-1}\left(\frac{ro}{r}\right) + Cos^{-1}\left(\frac{ro}{r}\right) - Cos^{-1}\left(\frac{ro}{R}\right)$$

$$p = 2Cos^{-1}\left(\frac{ro}{r}\right) \tag{3.2}$$

Putting the value of p in equation (1)

$$t(r) = \frac{Cos^{-1}\left(\frac{ro}{r}\right)}{\pi}.m_R.n_R.t_p \ (r_o \leq r \leq r_o + b) \tag{3.3}$$

3.2. Dome thickness outside of one-band width

Fiber tapes with b width cross at the Point A between points B, C, B' and C' in such a way that, the thickness at point A become equal to the sum of the thicknesses of these fiber tows passing over point A as shown in the figure 3.2.

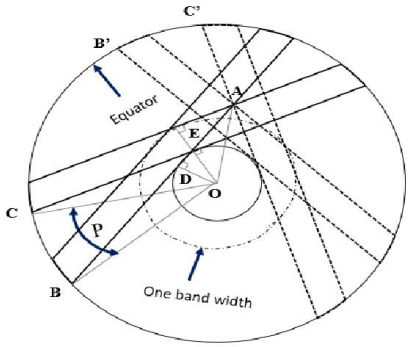

Figure 3.2: Pictorial correlation about fiber bands outside of one-band width.

Equation (3.3) becomes

$$t(r) = \frac{2p}{2\pi}.m_R.n_R.t_p \ (r_o + b \le r \le R) = \frac{p}{\pi}.m_R.n_R.t_p \qquad (r_o + b \le r \le R)$$

$$p = \angle BOC = \angle DOE = \angle AOD - \angle AOE = Cos^{-1}\left(\frac{ro}{r}\right) - Cos^{-1}\left(\frac{ro+b}{r}\right)$$

$$t(r) = \frac{Cos^{-1}\left(\frac{ro}{r}\right) - Cos^{-1}\left(\frac{ro+b}{r}\right)}{\pi}.m_R.n_R.t_p \ (r_o + b \le r \le R) \qquad (3.4)$$

3.2.A cubic spline function used to estimate thickness at dome portion

A cubic spline function $t(r_i)$ is presented to refine thickness on the basis of Equations (3.1) and (5), $t(r_i)$ has the following characteristics:

1. Function gives the thickness at arbitrary radius $t(r_i)$ in the interval [r_o,R].

$$t(r_i) = A \times r_i^o + B\, r_i^1 + Cr_i^2 + Dr_i^3 \qquad (3.5)$$

2. $t(r_i)$ is continuous and differentiable in close interval [r_o,R], $t(r_i) \in C^2$ [r_o,R].

If A, B, C, and D are found, then the thickness can be easily forecasted. Four equations are introduced in order to find out the four coefficients.

3.3.Equation (1): Thickness of the dome at pole.

As mentioned before, the quantities of fiber tows at the dome section are equal to that at the cylinder section because of the continuity of the filament winding process:

$$m_o.n_o = m_R.n_R \qquad (3.6)$$

Where m_o and n_o are the quantity of fiber tapes and the quantity of single plies at the pole of the dome, respectively.

Thickness of the laminates in the cylindrical section of the vessel is $t_R = 2n_R.t_p$ and $m_R = 2\pi R/(b/Cos\alpha_o)$, then Equation (7) can be expressed as:

$$n_o = m_R.\frac{n_R}{m_o} = t_R\,\pi R\frac{Cos\alpha_o}{m_o.b.t_p} \qquad (3.7)$$

Let take the thickness of the fiber at the pole of the radius r_o, the relationship between number of the fibers required to fill the mandrel for one helical session and radius of the cylindrical section, helical angle at the cylindrical section is given below:

$$\text{t}\,(r_o) = n_o.\, t_p = t_R\ \text{R}\ \pi \frac{Cos\ \alpha_o}{m_o.b} \tag{3.8}$$

The thickness of the fiber at the pole of the dome is calculated by following the equation (3.5), which is given below:

$$\text{t}\,(r_o) = n_o.\, t_p = t_R\ \pi\text{R}\frac{Cos\alpha_o}{m_o.b} = \text{A x}\ r_o^o + \text{B}\ r_o^1 + Cr_o^2 + Dr_o^3 \tag{3.9}$$

3.4. Equation (2): dome Thickness within the two-band width.

Fiber thickness within the two-band width can be expressed by equation (3.4):

$$\text{t}\,(r_{2b}) = \frac{Cos^{-1}\left(\frac{ro}{r_{2b}}\right) - Cos^{-1}\left(\frac{ro+b}{r_{2b}}\right)}{\pi}.m_R.\, n_R.\, t_p = \text{A x}\ r_{2b}^o + \text{B}\ r_{2b}^1 + Cr_{2b}^2 + Dr_{2b}^3 \tag{3.10}$$

3.5. Equation (3): Taking derivatives of Equations (3.4) and (3.5) in order to get smooth curve.

$$\frac{dt(r_{2b})}{dr} = \frac{m_R.\, n_R}{\pi}.\left(\frac{r_o}{r_{2b}\text{x}\sqrt{r_{2b}^2 - r_o^2}} - \frac{r_b}{r_{2b}\text{x}\sqrt{r_{2b}^2 - r_o^2}}\right) t_p = \text{B} + 2\ \text{x}\ Cr_{2b} + 3Dr_{2b} \tag{3.11}$$

3.6. Equation (4): The number of fiber tapes remain constant with in the two-band width.

$$\int_{r_o}^{r_{2b}} 2\pi\ x\ t(r_i)dr = \int_{r_o}^{r_b} 2\pi\ r\ \frac{m_R.\, n_R}{\pi}\ Cos^{-1}\left(\frac{ro}{r}\right) t_p dr +$$

$$\int_{r_b}^{r_{2b}} 2\pi\ r\ \frac{m_R.\, n_R}{\pi}\ \left[Cos^{-1}\left(\frac{r_o}{r_{2b}}\right) - Cos^{-1}\left(\frac{r_o+b}{r_{2b}}\right)\right] t_p dr \tag{3.12}$$

The coefficients A, B, C and D which are unknown can be now easily derived from equation could be solved from equations (3.9), (3.10), (3.11) and (3.12), which can be written in the form of matrix shown in the below equation:

$t(r_i)$ = A x r_i^o + B x r_i^1 +C x r_i^2 + D x r_i^3

$$\begin{bmatrix} 1 & r_o & r_o^2 & r_o^3 \\ 1 & r_{2b} & r_{2b}^2 & r_{2b}^3 \\ 0 & 1 & 2r_{2b} & 3r_{2b}^2 \\ \pi(r_{2b}^2 - r_o^2) & \frac{2\pi}{3}(r_{2b}^3 - r_o^3) & \frac{\pi}{2}(r_{2b}^4 - r_o^4) & \frac{2\pi}{5}(r_{2b}^5 - r_o^5) \end{bmatrix} \begin{bmatrix} A \\ B \\ C \\ D \end{bmatrix} =$$

$$\begin{bmatrix} t_R \pi . Cos\left(\frac{\alpha_o}{m_o b}\right) \\ \frac{Cos^{-1}\left(\frac{ro}{r_{2b}}\right) - Cos^{-1}\left(\frac{ro+b}{r_{2b}}\right)}{\pi} . m_R . n_R . t_p \\ \frac{m_R . n_R}{\pi} . \left(\frac{r_o}{r_{2b} \mathrm{x} \sqrt{r_{2b}^2 - r_o^2}} - \frac{r_b}{r_{2b} \mathrm{x} \sqrt{r_{2b}^2 - r_o^2}} \right) t_p \\ V_{const} \end{bmatrix} \quad (3.13)$$

V_{const} which is written in the equation (3.13) is the constant which depends upon number of the fiber required to fill the mandrel, number of helical sessions, angle at the arbitrary radius and thickness of used fiber, which can be suppressed as below equation:

$$V_{const} = \int_{r_o}^{r_b} 2\pi\, r \frac{m_R . n_R}{\pi}\, Cos^{-1}\left(\frac{ro}{r}\right) t_p dr +$$

$$\int_{r_b}^{r_{2b}} 2\pi\, r \frac{m_R . n_R}{\pi} \left[Cos^{-1}\left(\frac{r_o}{r_{2b}}\right) - Cos^{-1}\left(\frac{r_o + b}{r_{2b}}\right) \right] t_p dr$$

CHAPTER 4

4. ANALYTICAL MODELS AND NUMERICAL METHODOLOGY

In this chapter, a simplified analytical method is developed to find out the thickness of the laminates at anywhere of the vessel. Using this simplified analytical method, the dome thickness of an arbitrary composite pressure vessel is estimated. An approximated surface is developed which depends upon the helical angle and profile of the dome. Analytical model based on the approximated surface gives the accurate results. Then, the precision of simplified analytical method is deliberated for forecasting of the fiber thickness in the dome "A simplified analytical method for wound composite pressure vessel design".

4.1. Approximated surface at helical angle θ

Let consider a vessel whose total length is L_v and total cylindrical diameter is D_v and its dome with pole length is L_d and pole diameter is D_p as shown in the figure below.

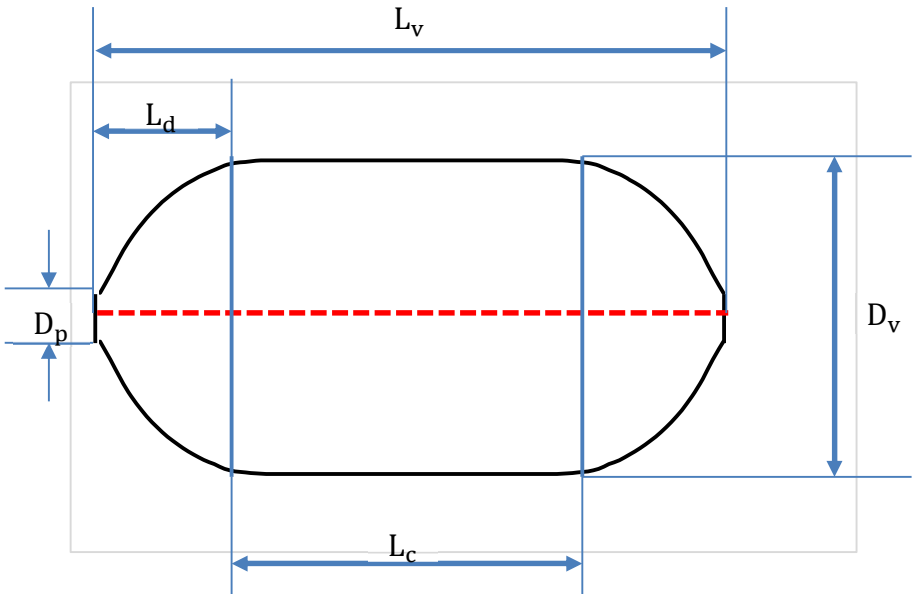

Figure 4.1: Profile of the vessel with dome

Continuous filament winding process is the process in which fiber wound over a mandrel passing tangent to the pole opening of the vessel which is normal to the meridian of the vessel. Variation of the helix angle totally depends upon the profile of the vessel. Helix angle relation is known as Clairant equation [11] which is validated by (Kaleem's work) is used to find out the helical angle at anywhere of the vessels. Helical path of fiber and various geometry of the vessel is given in the below figure in which fiber enters from cylindrical portion into the dome at Y point at θ_Y and helicl angles goes on increasing towards the pole and fiber becomes tangent at o point which is the pole of the vessel and this winding angle goes on decreasing as diameter of vessel increases and enters with the angle θ_H at H point which is located at the equator of the vessel. Fiber covers 2A arc length while passing through the dome as shown in the below figure.

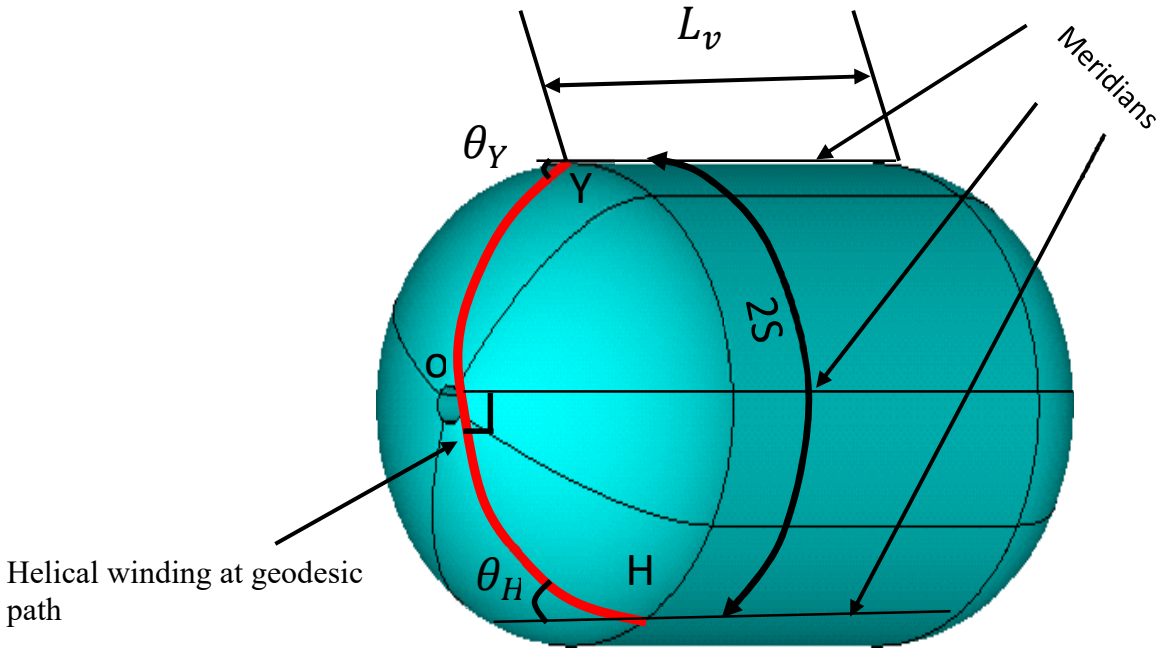

Figure 4.2: 3D of vessel with starting of the wound and parts labelling

Developed surface of figure 3.4 is shown in the figure 3.5 (a) in which horizontal lines are along the longitudinal axis and vertical lines represents the circumference of vessel. The development is seen in figure 3.5 (a) divided into three regions with the middle one representing cylindrical region while the two outer ones representing the two domes.

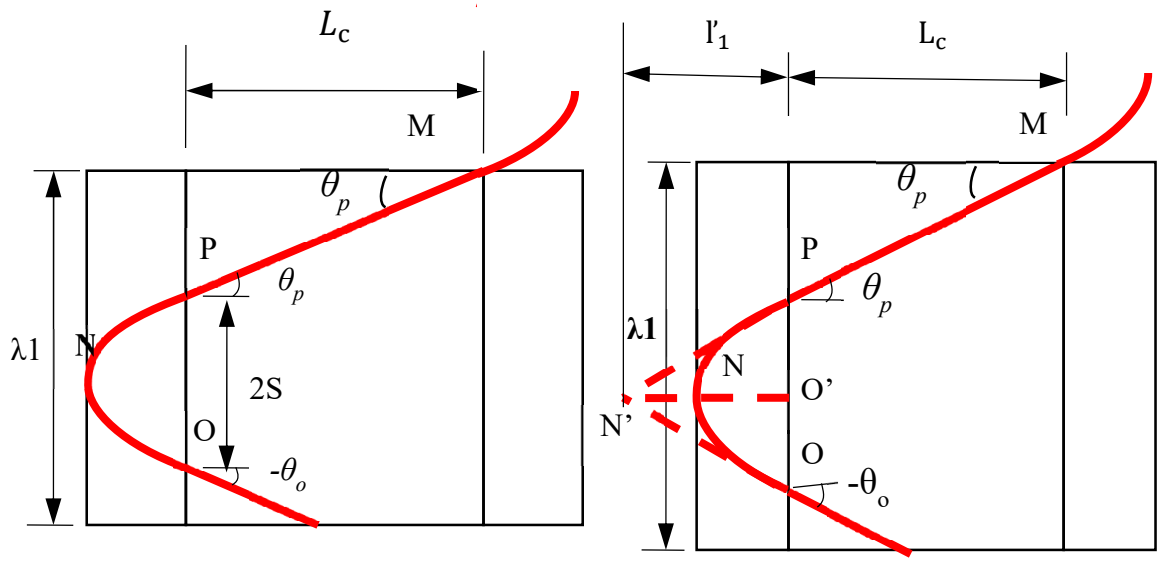

Figure 4.3: (a) Developed geometry of Fig. 3.4 (b) Development of Fig. 3.5 (a) redrawn with additional details

There is a specific helical angle θp at Point M. The angle θp is remains constant throughout the cylindrical region until it enters the other dome. It enters the dome region at point P and passes tangentially to the pole at point N and re-enters cylinder with helix angle $-\theta_0$ at point O with $|\theta_p| = |-\theta_0| = \theta_{en}$. For simplicity Curve PNO may be replaced by an isosceles triangle PN'O with N'O' being the height of the triangle and OP being its base (figure 3.5(b)). l' is length of fiber remains out of cylindrical portion in one dome which is equal to $S/\tan\theta_{en}$, L is total developed length of vessel which is mathematical equal to $L_c + 2\,l'$. $\lambda_1 = \pi D_c$ and $\lambda_2 = 2\,L\tan(\theta)$ are Wavelength of circumference repetition wave and Wavelength of triangular wave respectively.

Merging the circumferential development, we observe mosaic patterns as shown in figure 3.7 (a). Diamond ◇ cadb is taken which consists of two triangles △ bca and △ bad. Taking triangle △bca and draw l_{CL} normal line to the cd side. Equation to find length of l_{CL} is based on simple trigonometric laws.

Let's point 'a' is located at origin with 0,0 coordinates, point 'b' is located with 0, p_{CD} and point 'c' of triangle is located with $-{}^{q}/_{2}$, ${}^{p_{CD}}/_{2}$.

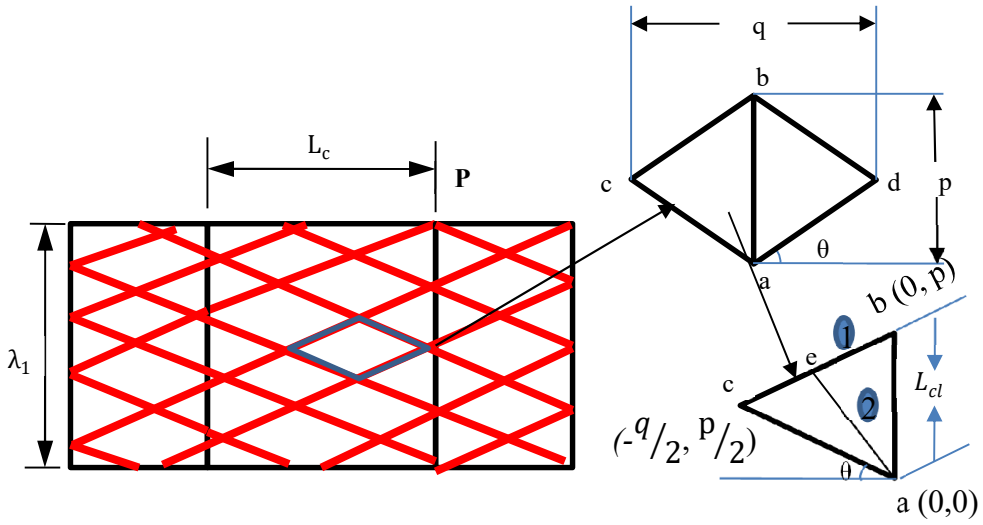

Figure 4.4: (a) Merging extended development of figure 4.3 (b) Diamond and triangular shape from figure 4.4(a) with additional details.

Straight-line equation of line bc

$$Y_{cb} = p - X_{cb} \tan(\theta) \quad (4.1)$$

Straight line equation of line l_{CL}

$$Y_{l_{CL}} = X_{l_{CL}} \tan(-(90+\theta))$$

$$Y_{l_{CL}} = -X_{l_{CL}} \tan(90+\theta) \quad (4.2)$$

To find out the intersection points of these lines. Equating equation, a and b and supposing $X_{cb} = X_{l_{CL}} = X$

$$p - X \tan\theta = -X \tan(90+\theta)$$
$$p = X(\tan\theta - \tan(90+\theta))$$

$$X = \frac{p}{(\tan\theta - \tan(90+\theta))}$$

$\therefore \tan(90+\theta) = -\cot\theta$

$$X = \frac{p}{\tan\theta + \cot\theta}$$

$$X = \frac{p_{CD}}{\frac{\sin\theta}{\cos\theta} + \frac{\cos\theta}{\sin\theta}}$$

$$X = \frac{p\cos\theta\sin\theta}{sin^2\theta + cos^2\theta}$$

$$X = p\cos\theta\sin\theta \tag{4.3}$$

Taking equation 8

$$Y = -X\tan(90+\theta)$$
$$Y = X\cot\theta$$

Putting value of X from equation 9

$$Y = X\cot\theta$$
$$Y = p\cos\theta\sin\theta\cot\theta$$
$$Y = p\cos\theta\sin\theta\frac{\cos\theta}{\sin\theta}$$

$$Y = p\cos\theta^2 \tag{4.4}$$

After finding out the intersection points of line bc and l_{CL}

Length of L_{normal} can be calculated

$$L_{normal} = \sqrt{X^2 + Y^2}$$

Putting values of X and Y from equations c and d respectively

$$L_{normal} = \sqrt{(L_{dc}\cos\theta\sin\theta)^2 + (L_{dc}cos^2\theta)^2}$$

$$L_{normal} = \sqrt{L_{dc}{}^2 cos^2\theta sin^2\theta + L_{dc}{}^2 cos^4\theta}$$

$$L_{normal} = p\cos\theta\sqrt{sin^2\theta + cos^2\theta}$$

$\therefore \sqrt{sin^2\theta + cos^2\theta} = 1$

$$L_{normal} = p \cos\theta \tag{4.5}$$

Normal line L_{normal}totally depends open the circumferential length of diamond and helix angle. This line consisted in the dome portion due to change of helix angle and circumferential length. Shrinkage of this line mean the concentration of fiber. Fiber thickness proportionally related to the shrinkage of the normal line.

4.2.Overlapping of fiber tapes

Whereas $l_g$unsupported region of first tape that is mathematically equal to $\frac{2(L_{nor}-W)}{N_f-1}$.
Number of tapes with which first tap overlaps is calculated as

$$\text{If} \begin{Bmatrix} n \geq N_f \\ then \\ n = N_f - 1 \end{Bmatrix} \tag{4.6}$$

This condition is introduced because first tap overlaps with available $N_f - 1$ taps that's why if n $\geq N_f$ then by putting n=$N_f - 1$.

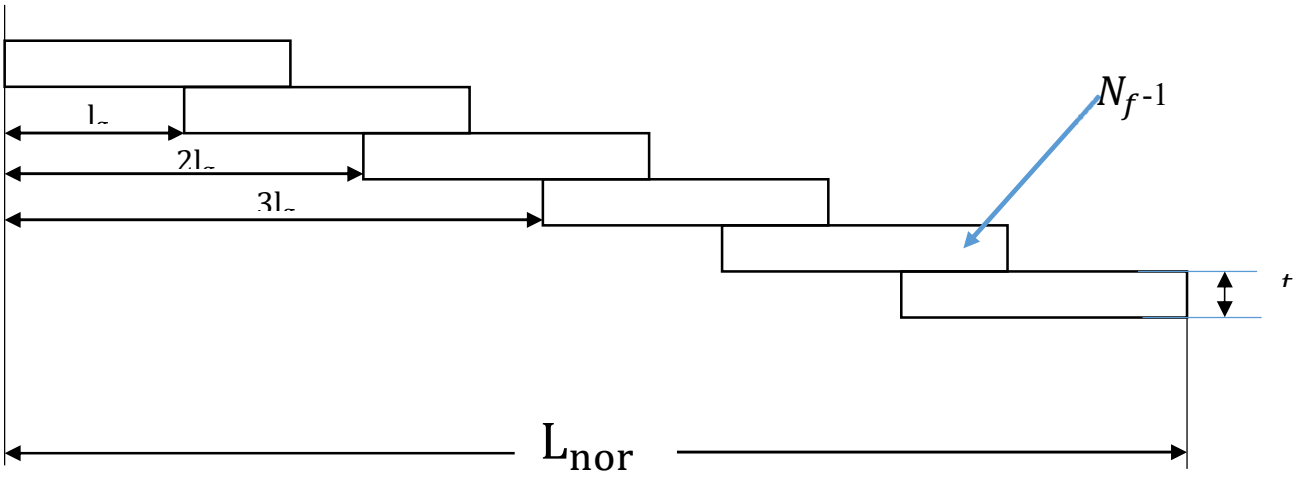

Figure 4.5: Overlapping within the L_nor

Increasing winding angle from equator to pole of vessel makes more overlapping of fiber taps that is responsible for increase in fiber thickness[1]. Moreover, two basic assumptions are taken into consideration for the finding out of thickness in the curvilinear portion of the vessels: It is fact that the number of the fiber tapes used to fill the cylindrical portion remains constant throughout the vessel [13].

Find out the situation at which maximum number of tapes are overlapped then multiply that specific number which the tape thickness gives the thickness of laminate given as

$$t_{ply} = (n_{maxi}+1) \text{ x } t_p \quad (4.7)$$

Thickness of fiber layer depends upon the geometry of the vessel and angle in the dome.
Flow chart of this research work is mentioned in figure 4.6.

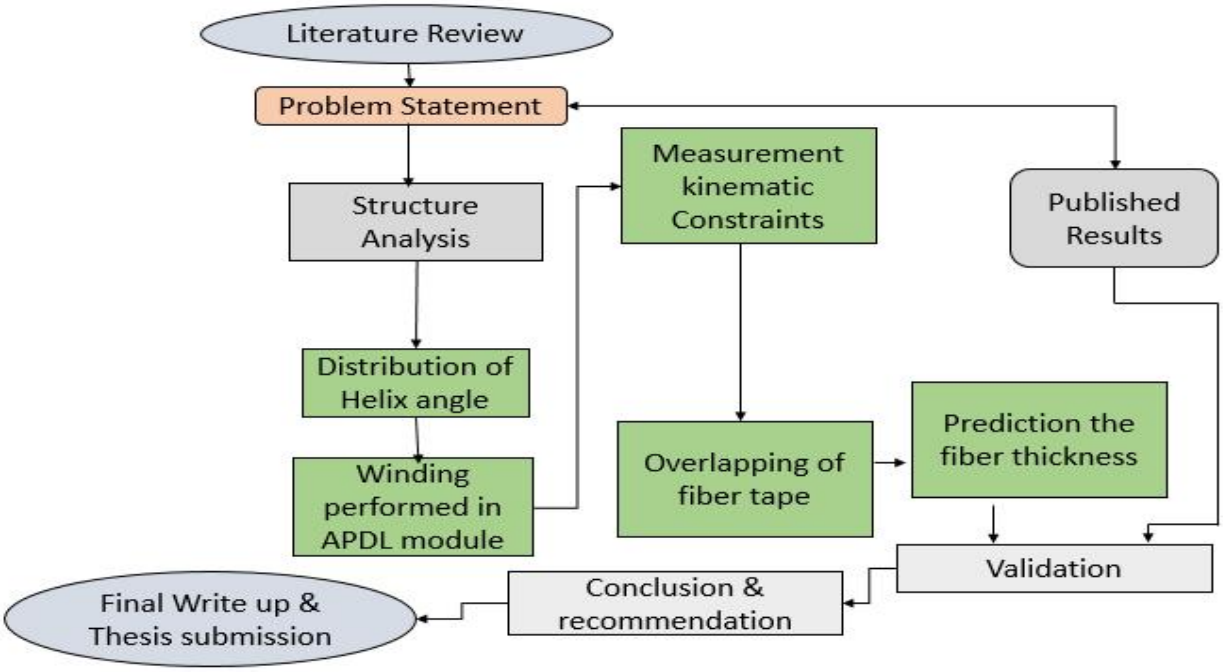

Figure 4.6: Procedure to find out the fiber thickness

CHAPTER 5

5. MECHANICS OF LAMINATED STRUCTURES

Laminates of composite structure are made from lamina or plies with same or varying thickness and containing two or more different materials, and each ply has a single fiber direction rather than a weave pattern[14]. These laminates are analytically modelled with the help of classical laminated plate theory (CPT) [15]. This theory predicts elastic properties like the strains, displacement and curvatures developed in a laminate as a result of mechanically or thermally loaded but with some assumptions like layers are properly buttered together to form laminates[16], laminate with its layers are in a state of plane stress, transverse shear strains are zero because traditional lines perpendicular to the central surface remain straight and perpendicular to that surface after distortion and traverse normal strain is zero because perpendicular distances from middle surface remain unchanged [17]. A multidirectional laminated plate is treated in xyz coordinate system assuming reference plane lies on the middle surface of the plate and an individual layer k is considered whose mid plane is at a distance y_k from the laminate reference plane[17] as shown in the figure 5.1.

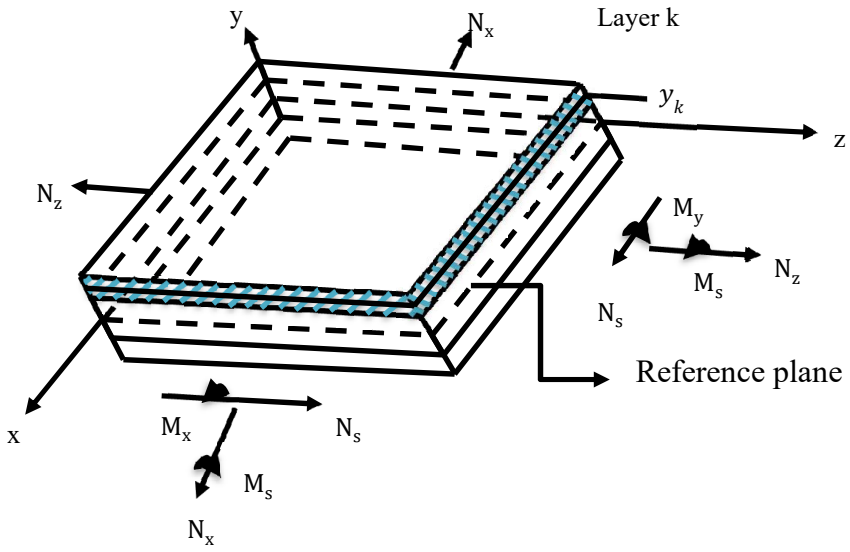

Figure 5.1: Layer 'k' in unidirectional laminated plate with force and moment results with coordinates system

It is supposed that the lamina is always in the two dimensional state of the and at this plane

stress state lamina compliance matrix is expressed as [18].

$$[S_{126}] = \begin{bmatrix} \frac{1}{E_1} & -\frac{v_{12}}{E_1} & 0 \\ -\frac{v_{12}}{E_1} & \frac{1}{E_2} & 0 \\ 0 & 0 & \frac{1}{G_{12}} \end{bmatrix} \tag{4.1}$$

Whereas E_1,E_2,G_{12},$v_{12}$and v_{21} are engineering properties of the fiber used to make the pressure vessel.
Lamina Modulus matrix is calculated as:

$$[Q_{126}] = [S_{126}]^{-1} \tag{4.2}$$

The components of lamina modulus matrix are

$$Q_{11} = \frac{E_1}{1-v_{12}v_{21}}$$

$$Q_{12} = Q_{21} = \frac{v_{12}E_2}{1-v_{12}v_{21}} \tag{4.3}$$

$$Q_{22} = \frac{E_2}{1-v_{12}v_{21}}$$

$$Q_{66} = Q_{12}$$

The lamina axes (1,2) do not correspond to the global axes (z, x) shown in the figure 5.2.

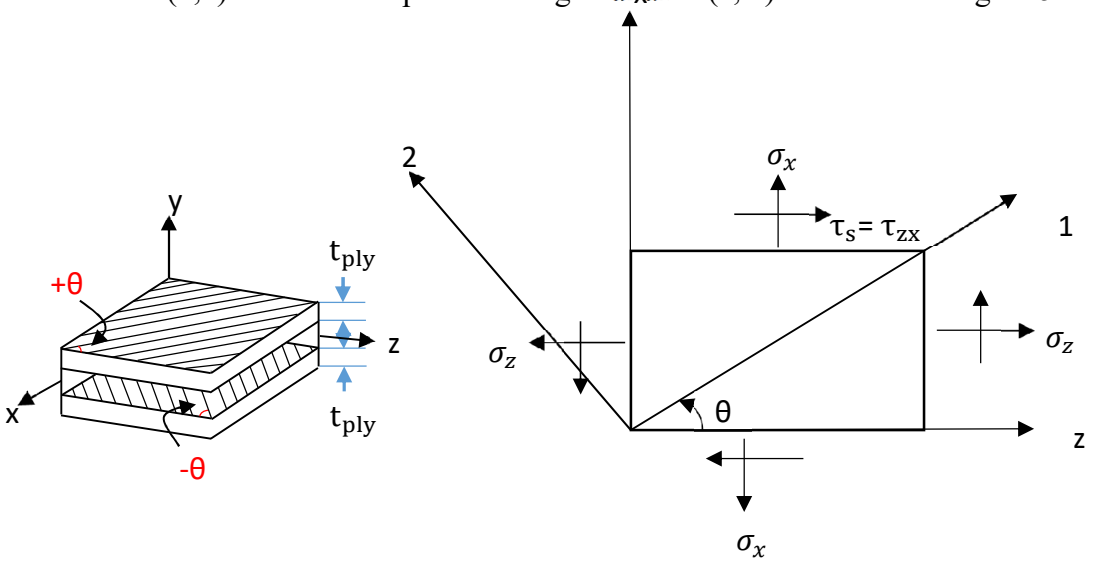

Figure 5.2: Ant-symmetric angle ply layer and stress composites in unidirectional lamina referred to loading and material axis

$$[T] = \begin{bmatrix} \cos^2\theta & \sin^2\theta & 2\sin\theta\cos\theta \\ \sin^2\theta & \cos^2\theta & -2\sin\theta\cos\theta \\ -\sin\theta\cos\theta & \sin\theta\cos\theta & \cos^2\theta - \sin^2\theta \end{bmatrix} \quad (4.4)$$

Inverse of transformation matrix is calculated as

$$[T]^{-1} = \begin{bmatrix} \cos^2\theta & \sin^2\theta & -2\sin\theta\cos\theta \\ \sin^2\theta & \cos^2\theta & 2\sin\theta\cos\theta \\ \sin\theta\cos\theta & -\sin\theta\cos\theta & \cos^2\theta - \sin^2\theta \end{bmatrix} \quad (4.5)$$

Reuter Matrix

$$[R] = \begin{bmatrix} 1 & 0 & 0 \\ 0 & 1 & 0 \\ 0 & 0 & 2 \end{bmatrix} \quad (4.6)$$

Inverse of Reuter Matrix

$$[R]^{-1} = \begin{bmatrix} 1 & 0 & 0 \\ 0 & 1 & 0 \\ 0 & 0 & 0.5 \end{bmatrix} \quad (4.7)$$

Lamina Global Modulus matrix

$$[Q_{zxs}] = [T]^{-1}[Q]_{126}[R][T][R]^{-1} \quad (4.8)$$

Lamina Global Compliance matrix

$$[S_{zxs}] = [Q_{zxs}]^{-1} \quad (4.9)$$

As stresses do not vary linearly through thickness direction from layer to layer as strains do so it is more appropriate to take the combined consequence of these discontinuous stresses on the laminate. The force and moment resultants for the N_{ply} are obtained as [17].

$$\begin{bmatrix} N_z \\ N_x \\ N_s \end{bmatrix} = \int_{y_{k-1}}^{y_k} \begin{bmatrix} \sigma_z \\ \sigma_x \\ \sigma_s \end{bmatrix} dy = \sum_{k=1}^{N_{ply}} [Q_{zxs}]^k \left\{ \int_{y_{k-1}}^{y_k} [\varepsilon^0]_{zxs}\, dy + \int_{y_{k-1}}^{y_k} [k]_{zxs} y\, dy \right\} \quad (4.10)$$

$$\begin{bmatrix} M_z \\ M_x \\ M_s \end{bmatrix} = \int_{y_{k-1}}^{y_k} \begin{bmatrix} \sigma_z \\ \sigma_x \\ \sigma_s \end{bmatrix} y dy = \sum_{k=1}^{N_{ply}} [Q_{zxs}]^k \left\{ \int_{y_{k-1}}^{y_k} [\varepsilon^0]_{zxs} y\, dy + \int_{y_{k-1}}^{y_k} [k]_{zxs} y^2\, dy \right\} \quad (4.11)$$

Whereas $[\varepsilon^0]_{zxs}$, $[k]_{zxs}$, y_k and y_{k-1} are the mid surface strains, curvatures, upper and lower surfaces of layer k in y direction respectively. The lamina global modulus matrix can be further specified as

$$[Q_{zxs}]=\begin{bmatrix} Q_{zz} & Q_{zx} & Q_{zs} \\ Q_{zx} & Q_{xx} & Q_{xs} \\ Q_{zs} & Q_{xs} & Q_{ss} \end{bmatrix} \tag{4.12}$$

$$\begin{aligned}
Q_{zz} &= Q_{11}\cos^4\theta + 2(Q_{12}+2Q_{66})\cos^2\theta\sin^2\theta + Q_{22}\sin^4\theta \\
Q_{zx} &= (Q_{11}+Q_{22}-4Q_{66})\cos^2\theta\sin^2\theta + Q_{12}(\sin^4\theta+\cos^4\theta) \\
Q_{xx} &= Q_{11}\sin^4\theta + 2(Q_{12}+2Q_{66})\cos^2\theta\sin^2\theta + Q_{22}\cos^4\theta \\
Q_{zs} &= (Q_{11}-Q_{12}-2Q_{66})\cos^3\theta\sin\theta + (Q_{12}-Q_{22}+2Q_{66})\sin^3\theta\cos\theta \\
Q_{xs} &= (Q_{11}-Q_{12}-2Q_{66})\sin^3\theta\cos\theta + (Q_{12}-Q_{22}+2Q_{66})\cos^3\theta\sin\theta \\
Q_{ss} &= (Q_{11}+Q_{22}-2Q_{12}-2Q_{66})\cos^2\theta\sin^2\theta + Q_{66}(\cos^4\theta+\sin^4\theta)
\end{aligned} \tag{4.13}$$

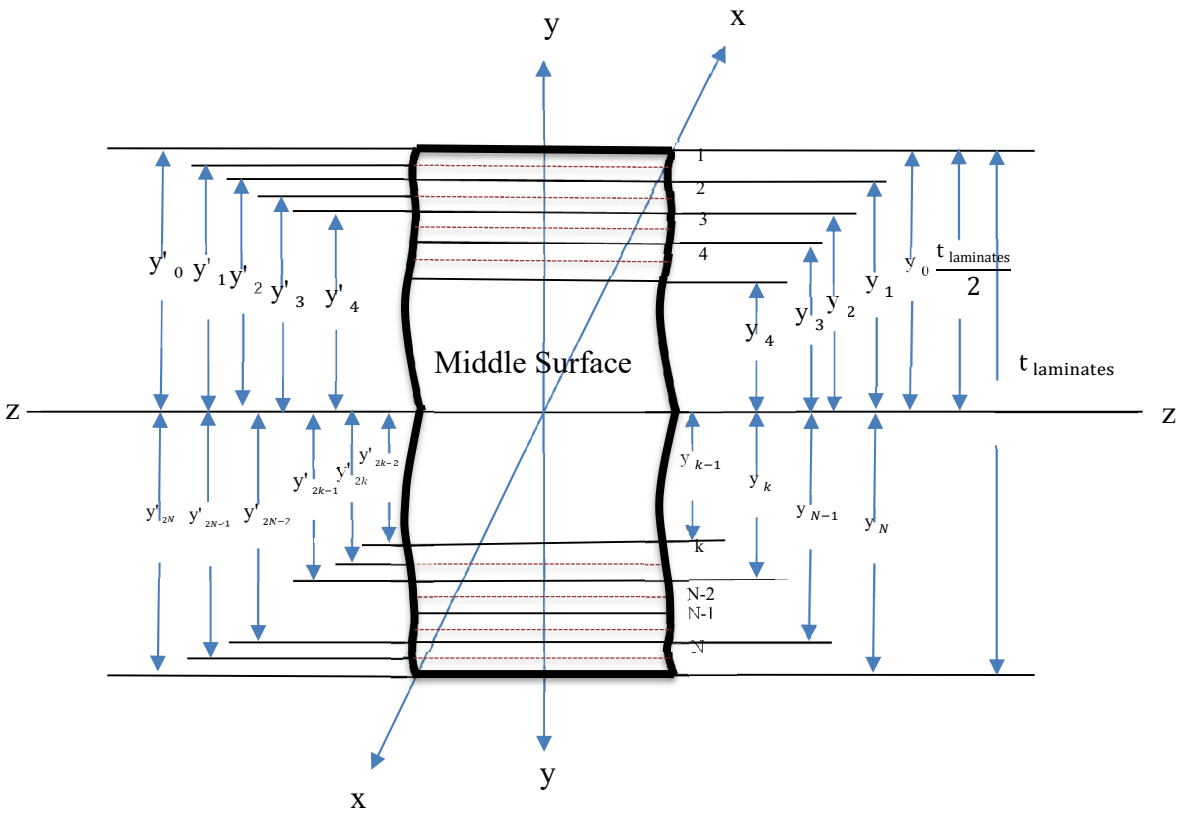

Figure 5.3: Laminated plate geometry and ply numbering system, y_k and y'_{2k} are distance of individual layer k and middle surface distance of k ply from the laminate reference respectively

Above relation can be written in the form of three laminate stiffness matrices named [A], [B] and [D]

$$[A_{ki}]= \sum_{k=1}^{N_{ply}} [Q_{ki}]^k (y_k - y_{k-1}) \quad (4.14)$$

$$[B_{ki}]= \frac{1}{2} \sum_{k=1}^{N_{ply}} [Q_{ki}]^k (y_k^2 - y_{k-1}^2) \quad (4.15)$$

$$[D_{ki}]= \frac{1}{3} \sum_{k=1}^{N_{ply}} [Q_{ki}]^k (y_k^3 - y_{k-1}^3) \quad (4.16)$$

Where:

$[A_{ki}]$= Laminate extensional stiffness or in-plane laminate moduli.

$[B_{ki}]$= Laminate coupled bending-extension stiffness.

$[D_{ki}]$= Laminate bending or flexural stiffness.

y_k = Distance of individual layer k from the laminate to reference.

The overall load-deformation relations for this class of laminates are:

$$\begin{Bmatrix} \varepsilon^0_{zxs} \\ k_{zxs} \end{Bmatrix} = \begin{bmatrix} A & B \\ B & D \end{bmatrix}^{-1} \begin{Bmatrix} N \\ M \end{Bmatrix} \quad (4.17)$$

Where as ε^0_{zxs} and $k_{zxs}$the mid surface strains and curvatures.

Relationship between strain at any point y in the laminates to the reference planes strains and the laminate curvature is given as [17]

$$\begin{bmatrix} \varepsilon_z \\ \varepsilon_x \\ \gamma_s \end{bmatrix} = \begin{bmatrix} \varepsilon_z^0 \\ \varepsilon_x^0 \\ \gamma_s^0 \end{bmatrix} + y \begin{bmatrix} k_z \\ k_x \\ k_s \end{bmatrix} \quad (4.18)$$

The plane stress constitutive equation is given by:

$$\{\sigma_{zxs}\} = [Q_{zxs}]\{\varepsilon_{zxs}\} \quad (4.19)$$

The Lamina stresses in local co-ordinates

$$\{\sigma_{zxs}^0\} = [T]\{\sigma_{zxs}\}$$

CHAPTER 6

6. Filament wound structure modelling and FEA

The vessels have following parameters: r_c=66 mm radius of a cylindrical part; r_o= 9.5 mm radius of the polar (the same for both domes); L_c =100mm cylinder length; L = 260 mm total vessel length and distribution of radius corresponding to the length [7].

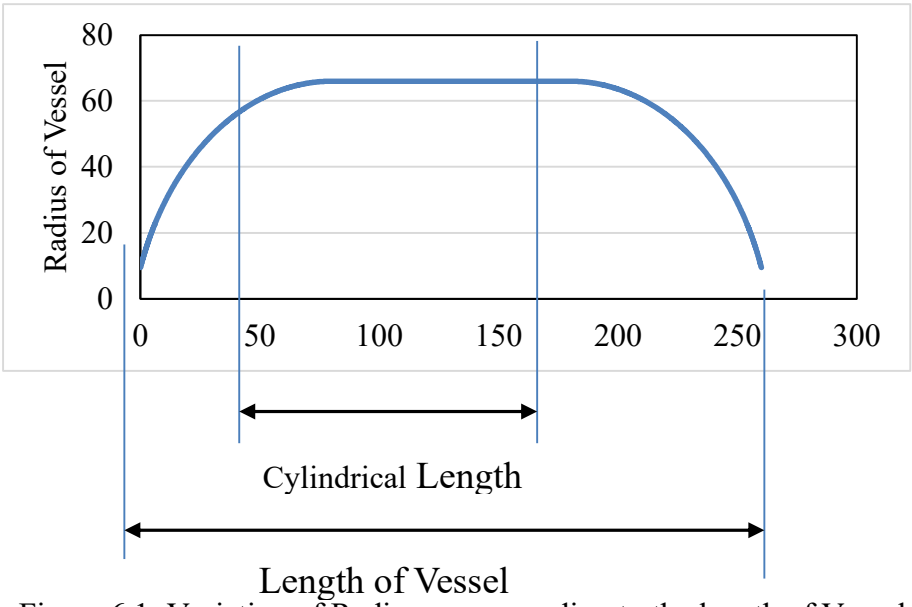

Figure 6.1: Variation of Radius corresponding to the length of Vessel

6.1. Splitting of vessels into small segments and generating geodesic path using APDL module of ANSYS

Dome of the vessel is divided into 38 small segments as shown 6.2 (a) in the figure in order to get accurate geodesic path with accurate helical angle as shown in the figure 6.2 (b).

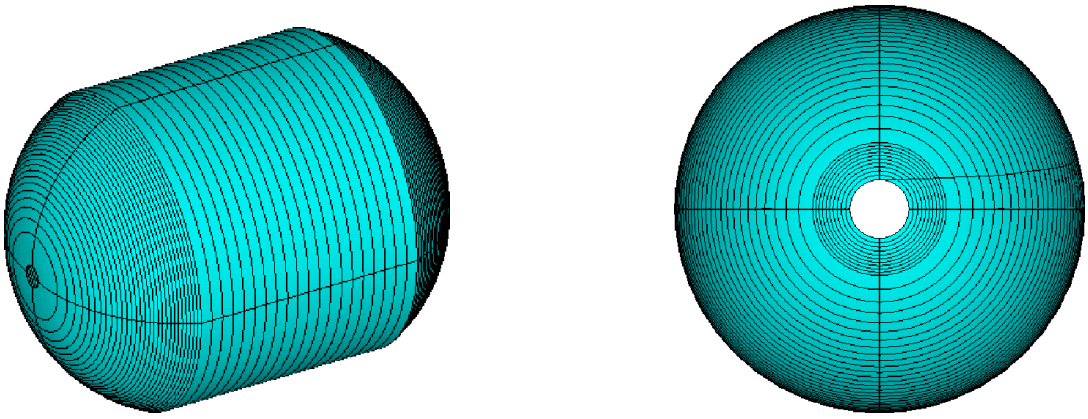

Figure 6.2: (a) Vessel with small segments (b) Vessel with Geodesic path

6.2. Helical angle and half the arc length

Dome is divided into 38 equally length segments, 8.425^0 helix angle is found that remains constant throughout the cylinder and fiber covers 86.06 mm half the arc length in dome portion.

6.3.Claurant's Equation [7]

$$\frac{Sin\theta c}{r_o} = \frac{Sin\,\theta o}{L_d}$$

$$\theta c = Sin^{-1}\left(\frac{r_o}{r_d} Sin\theta_o\right)$$

$$\theta c = Sin^{-1}\left(\frac{9.5}{66} Sin90\right)$$

$$\theta c = 8.25 \cong 8.425$$

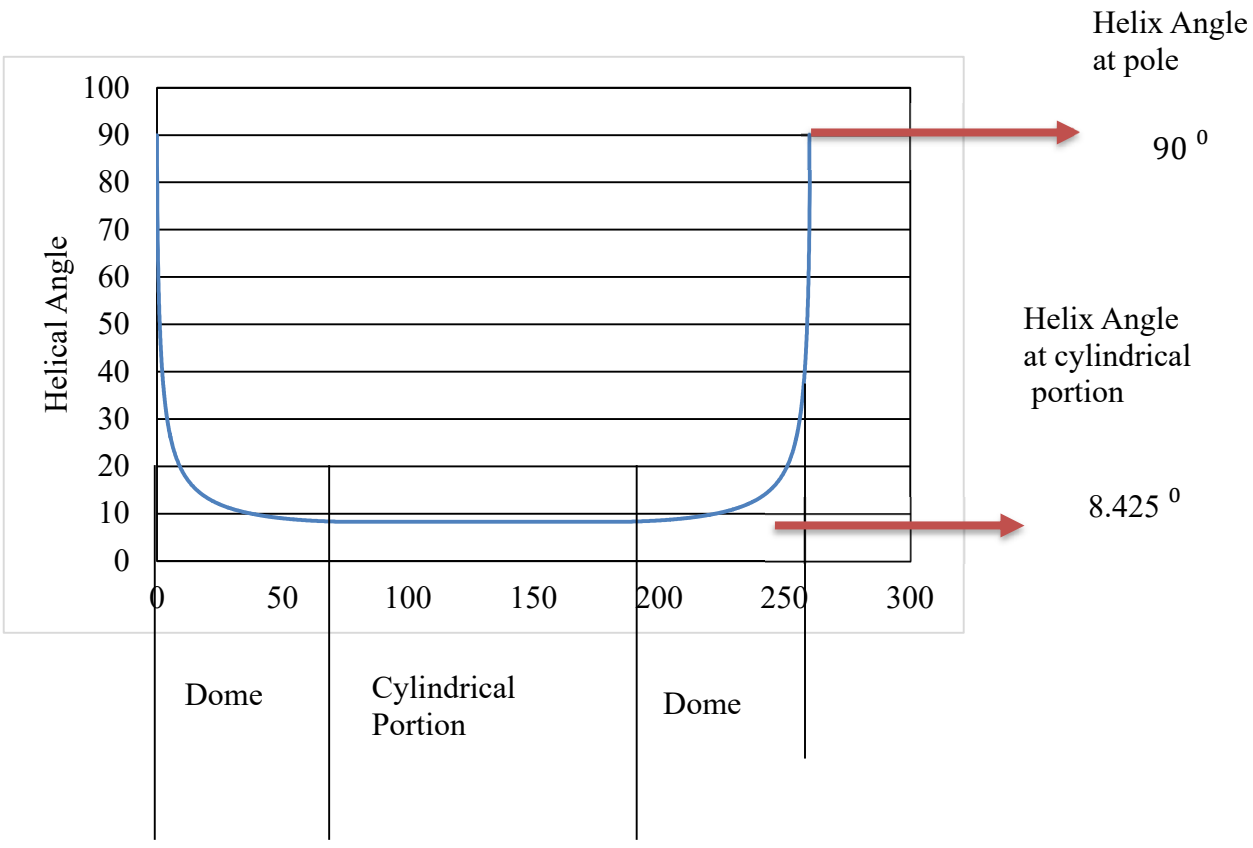

Figure 6.3: Variation of Helical angle corresponding to the length of Vessel

6.4. Dimensions of mosaic pattern and number of fibers required to fill the mandrel for one helical session

Fiber tap used for this research is 5.39mm wide and 0.765mm thick. At 10th trips gape (G_f) between starting and ending of fiber reaches 2.3437 mm. Analytical solution gives 10 repetition of circumferential wave (N_{cir}) and gape between starting and ending point of fiber is shown in the figure 6.4.

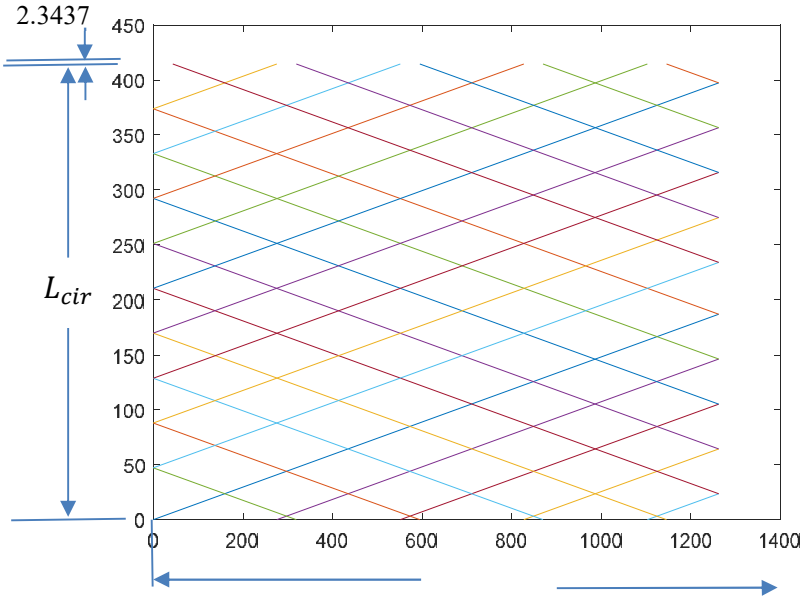

Figure 6.4: Filament winding pattern in MATLAB

At this condition number of cicumferential diamonds (N_{cir})= 10

Gape between starting and ending point of fiber tape after one complete helical session

G_f = 2.3437mm

Number of fiber tape required to fill the diamond formed is $N_f = \frac{\pi D_c \, Cos\theta_c}{N_{cir} G_f}$

$N_f = \frac{\pi 132 \, Cos 8.425}{10 \, (2.3437)}$ =17.42≅ 18

Dome thickness is required at below radius

Table 6-1: Relative error between the prediction values and actual values within two-band width

r (mm)	Actual measured thickness (mm)	Gramoll and Namiki's methods		The cubic spline function	
		Prediction values (mm)	Relative errors (%)	Prediction values (mm)	Relative errors (%)
11.57	23	22.53	2.04	24.05	−4.57
13.40	27.4	29.13	−6.31	28.42	−3.72
14.51	27.3	31.93	−16.96	27.28	0.07
15.75	25.0	22.19	11.24	24.0	4
16.62	20.0	18.79	6.05	21.04	−5.2
17.51	18.7	16.58	11.34	18.0	3.74
19.47	13.7	13.49	1.53	13.38	2.34

It is required to find out the helical angle at the given radius and then find out the L_{nor}

Length at this radius. Pole radius $(r_o) = 9.5\ mm$

Table 6-2: Normal length (L_nor) and gape in overlapping (l_g) at required radius

Sr. No	r	Helical Angle $(Sin^{-1}(\frac{r_o}{r}Sin90)$ at r	N_{cir}	L_{nor}	l_g (for first tape)
01	11.57	55.19396	10	4.149514714	0.359333333
02	13.4	45.14997	10	5.937859443	0.064454052
03	14.51	40.89849	10	6.891199316	0.176611684
04	15.75	37.0976	10	7.893153855	0.294488689
05	16.62	34.86191	10	8.568532562	0.373945007
06	17.51	32.8572	10	9.241839425	0.453157579
07	19.47	29.20463	10	10.6782896	0.622151718

After finding out the normal length and gape length in overlapping condition, it become easy to find out the dome thickness at the required radius.

Table 6-3: Dome thickness at the required radius

Sr. No	r (mm)	Number of tapes with ist tape n_{maxi}	tp	$t_{ply=(n+1)tp}$	$t_{lainates}$ = 2x t_p
01	11.57	14	0.765	11.475	**22.95**
02	13.4	17	0.765	13.77	**27.54**
03	14.51	17	0.765	13.77	**27.54**
04	15.75	16	0.765	13.05	**26.01**
05	16.62	13	0.765	10.71	**21.42**
06	17.51	11	0.765	9.18	**18.4**
07	19.47	8	0.765	6.885	**13.8**

It is clear from the table 6-3 that the dome thickness gradually decreases from the pole to the equator.

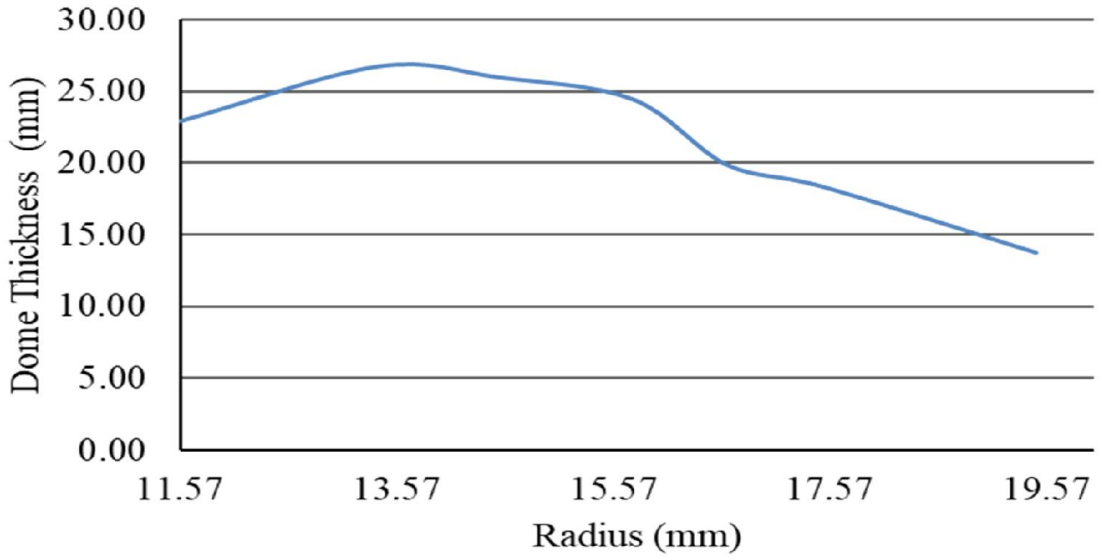

Figure 6.5: Variation of dome thickness corresponding radius

Table 6-4: Comparison with cubic spline function and Gramoll and Namiki's Method

			Analytical Method		Gramoll and Namiki Method		Cubic Spline Function	
Sr. No	r	Actual Thickness	Predicted Value	Relative error %	Predicted Value	Relative error %	Predicted Value	Relative error %
1	11.57	23	22.95	**0.22**	22.53	2.04	24.05	-4.57
2	13.4	27.4	26.78	**2.28**	29.13	-6.31	28.42	-3.72
3	14.51	27.3	26.01	**4.73**	31.93	-16.96	27.28	0.07
4	15.75	25	24.48	**2.08**	22.19	11.24	24	4.00
5	16.62	20	19.89	**0.55**	18.79	6.05	21.01	-5.05
6	17.51	18.7	18.36	**1.82**	16.58	11.34	18	3.74
7	19.47	13.7	13.77	**-0.51**	13.49	1.53	13.38	2.34

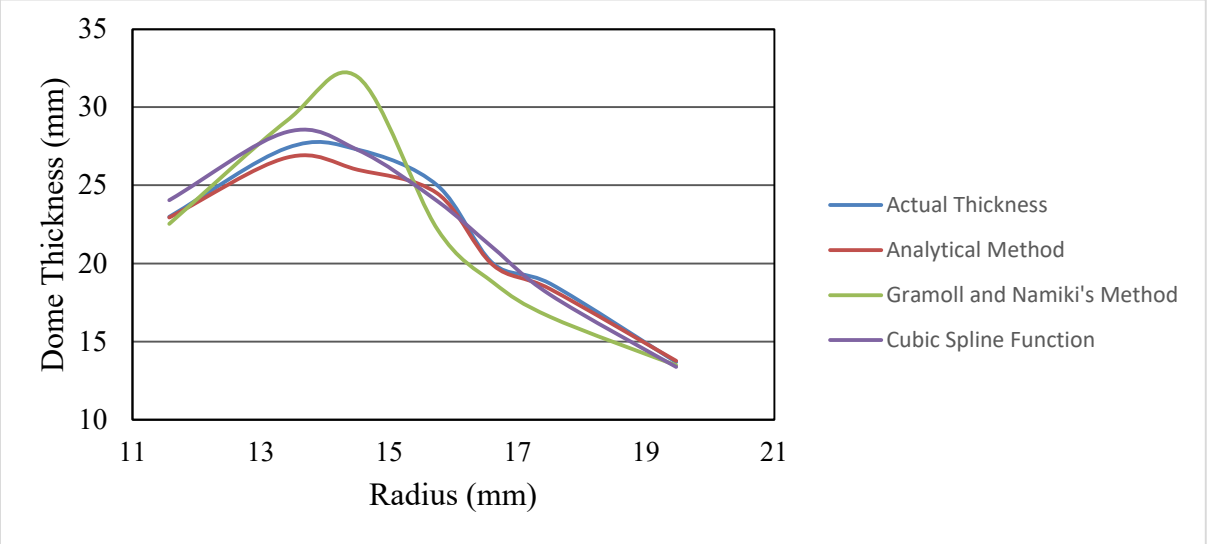

Figure 6.6: Variation of dome thickness corresponding radius with comparison of different methods

CHAPTER 7

7. CONCLUSION

- Analytical method gives optimum solution to find out the dome thickness.
- It gives the theoretic value by considering the kinematic constraints which totally depends upon the dome profile.
- This method gives the concept that decrement of dome thickness is smooth from pole to cylindrical section but cubic spline method gives an abrupt change in the dome thickness.
- This method gives the accurate result as compare to other methods i.e., cubic spline function and Gramoll and Nimiki method.

7.2. Future recommendation

Research work should extend to the investigation of the effect of the mosaic patterns on the mechanical behavior of the composite pressure vessels.

REFERENCES

[1] R. Wang, W. Jiao, W. Liu, and F. Yang, "A new method for predicting dome thickness of composite pressure vessels," *J. Reinf. Plast. Compos.*, vol. 29, no. 22, pp. 3345–3352, 2010.

[2] L. Zu, S. Koussios, and A. Beukers, "Shape optimization of filament wound articulated pressure vessels based on non-geodesic trajectories," *Compos. Struct.*, vol. 92, no. 2, pp. 339–346, 2010.

[3] V. V. Vasiliev and E. Morozov, *CH4 Advanced Mechanics of Composite Materials: Mechanics of a Composite Layer*. 2013.

[4] T. D. Canonsburg, "ANSYS Mechanical APDL Element Reference," vol. 15317, no. November, pp. 724–746, 2013.

[5] P. G. J. Z. X. X. X. Chen, "Winding angle optimization of filament-wound cylindrical," *Arch. Appl. Mech.*, vol. 87, no. 3, pp. 365–384, 2017.

[6] V. V. Vasiliev, A. A. Krikanov, and A. F. Razin, "New generation of filament-wound composite pressure vessels for commercial applications," *Compos. Struct.*, vol. 62, no. 3–4, pp. 449–459, 2003.

[7] B. J. Berenberg and J. W. Mar, "Mechanics of Filament Winding," in *Effect of Interweaving on the Axial Compressive Strength and Modulus of Filament-Wound Composite Cylinders*, 1991, p. 25.

[8] B. J. Berenberg and J. W. Mar, "Effect of Interweaving on the Axial Compressive Strength and Modulus of Filament-Wound Composite Cylinders by LIBi-Aero Aero," 1991.

[9] W. C. Chao and J. N. Reddy, "Analysis of laminated composite shells using a degenerated 3-D element," *Int. J. Numer. Methods Eng.*, vol. 20, no. 11, pp. 1991–2007, 1984.

[10] L. Nair, Y. Arasu, and V. S. Indu, "Design of Laminated Pressure Vessel," vol. 4, no. 8, pp. 1196–1202, 2015.

[11] A. A. Krikanov, "Composite pressure vessels with higher stiffness," *Composite Structures*, vol. 48, no. 1. pp. 119–127, 2000.

[12] I. To and C. Materials, *INTRODUCTION TO COMPOSITE MATERIALS*, no. August. 1984.

[13] J. S. Park, C. S. Hong, C. G. Kim, and C. U. Kim, "Analysis of filament wound composite structures considering the change of winding angles through the thickness direction," *Compos. Struct.*, vol. 55, no. 1, pp. 63–71, 2002.

[14] D. Dp, "Composite Materials 0," no. 5, p. 125, 1972.

[15] C. W. Bert, "A Critical Evaluation of New Plate Theories Applied to Laminated Composites *," vol. 2, pp. 329–347, 1984.

[16] C. T. Herakovich, "Mechanics of composites : A historical review," *Mech. Res. Commun.*, vol. 41, pp. 1–20, 2012.

[17] I. M. Daniel, *ENGINEERING MECHANICS OF COMPOSITE MATERIALS Ori lshai*. 2006.

[18] Gibson Ronald F, "Principles of Composite Material Mechanics," in *McGraw-Hill, Inc.*, no. 205, 1994, pp. xxvii, 579 p.

Annex A

%%% Input required%%

%% this code required radii and length of slices.

% Which give the Helix angle and Half Arc Length for which fiber remain out of cylinder%%%

R (1) =9.5;

R (2) =10.9605;

R (3) =12.34359;

R (4) =13.65928;

R (5) =14.9154;

R (6) =16.11836;

R (7) =17.27346;

R (8) =18.38517;

R (9) =19.45724;

R (10) =20.49292;

R (11) =21.49501;

R (12) =26.07761;

R (13) =30.08956;

R (14) =33.66173;

R (15) =36.87869;

R (16) =42.46471;

R (17) =44.90806;

R (18) =47.15363;

R (19) =49.220982;

R (20) =51.12591;

R (21) =52.88135;

R (22) =54.49803;

R (23) =55.98493;

R (24) =57.34966;

R (25) =58.59866;

R (26) =59.73745;

R (27) =60.77077;

R (28) =61.70266;

R (29) =62.53661;

R (30) =63.2756;

R (31) =63.92217;

R (32) =64.47848;

R (33) =64.94632;

R (34) =65.32716;

R (35) =65.62219;

R (36) =65.83229;

R (37) =65.9581;

R (38) =66;

L (1) =0.53333333333333333333333333333333;

L (2) =0.53333333333333333333333333333333;

L (3) =0.53333333333333333333333333333333;

L (4) =0.53333333333333333333333333333333;

L (5) =0.53333333333333333333333333333333;

L (6) =0.53333333333333333333333333333333;

L (7) =0.53333333333333333333333333333333;

L (8) =0.53333333333333333333333333333333;

L (9) =0.53333333333333333333333333333333;

L (10) =0.53333333333333333333333333333333;

L (11) =2.66666;

L (12) =2.66666;

L (13) =2.66666;

L (14) =2.66666;

L (15) =2.66666;

L (16) =2.66666;

L (17) =2.66666;

```
L (18) =2.66666;
L (19) =2.66666;
L (20) =2.66666;
L (21) =2.66666;
L (22) =2.66666;
L (23) =2.66666;
L (24) =2.66666;
L (25) =2.66666;
L (26) =2.66666;
L (27) =2.66666;
L (28) =2.66666;
L (29) =2.66666;
L (30) =2.66666;
L (31) =2.66666;
L (32) =2.66666;
L (33) =2.66666;
L (34) =2.66666;
L (35) =2.66666;
L (36) =2.66666;
L (37) =2.66666;
L (38) =2.66666;
n=38; %no of slices%
%%%% calculation%%%%
for i=1: n-1
  Phi(i)=acos((L(i)/(R(i+1)-L(i)))) *180/pi;
  ro(i)=(L(i+1))/cos (Phi(i)*pi/180);
  ri(i)=ro(i)-R(i)/sin (Phi(i)*pi/180);
end
%%% statig angle %%%%
Helix (1) =90;
Helix (2) =atan (ri (1) *sin ((180-Helix (1)) *pi/180)/ro (1)) *180/pi;
```

```
Arc_angle (1) =180-(180-Helix (1))-Helix (2);
Arc (1) =Arc_angle (1) *pi/180*ro (1);
for i=1: n-2
y(1+2*i) =x(1+2*i) *cos((90-Helix(1+i)) *pi/180) +ri(1+i);
y(2+2*i) =x(2+2*i) *cos((90-Helix(1+i)) *pi/180) +ri(1+i);
E(1+i) =power(power(x(1+2*i),2) +power((y(1+2*i)-ri(1+i)),2),.5);
Helix(2+i) =atan(ri(1+i) *sin((180-Helix(1+i)) *pi/180)/ro(1+i)) *180/pi
Arc_angle(1+i) =180-(180-Helix(1+i))-Helix(2+i);
Arc(1+i) =Arc_angle(1+i) *pi/180*ro(1+i);
end
%% final Out put%%
Helix_angle=Helix(n)
Half_the_Arc =sum (Arc)
```

Annex B

```
clc
clear all

l_cyl= 50; % Length of cylindrical portion alone
Max_Dia=145; % Dia of Cylindrical portion
c=pi*Max_Dia; % Circumference

angle=35;
Arc_length=847; %Half arclength for which fiber remains out of cylinder
alpha=angle*pi/180; % angle of winding in degree
Ext_Left=Arc_length/tan(alpha);
Ext_Right=Ext_Left;
l=Ext_Left+Ext_Right+l_cyl;

y2=0; y1=0; x2=0, x1=0, m=tan(alpha);

Coords=[];

for i=1:1000

% Meridian Check
x1=x2;
if y2==c
   y1=0;
else
   if y2==0
      y1=c;
   end
   y1=y2;
end

y3=c;
x3=((y3-y1)/m) +x1
if x3>0 && x3<l
   x2=x3;
```

```
    y2=y3;
    check=000000
else
    if x1==0
        x2=l;
    else
        if m>0
            x2=l;
        end
        if m<0
            x2=0;
        end
    end
    y2=m*(x2-x1) +y1;
end

% Slope Switch Check
if x2==l | x2==0
    m=-m;
end

    a= [x1 x2];
    b= [y1 y2];
    plot (am)
    hold on
    pause

Coords= [Coords; x1 y1; x2 y2]
end
```

Annex C

```
clc
clear all

l_cyl= 150;   % Length of cylindrical portion alone
Max_Dia=132; % Dia of Cylindrical portion
c=pi*Max_Dia; % Circumference

angle=8.9816;
Arc_length=43.44365; %Half arclength for which fiber remains out of
cylinder
alpha=angle*pi/180; % angle of winding in degree
Ext_Left=Arc_length/tan(alpha);
Ext_Right=Ext_Left;
l=Ext_Left+Ext_Right+l_cyl;


Lam1=c; % Cyl Lambda: Wavelength of Circumference Repitition Wave
Lam2=2*tan(alpha)*l; % Trig Lambda: Wavelength of Triangular Wave
ratio=Lam2/Lam1;
Tol=5.39; % Roving Width parallel to Circumference

n1=1:1:2000;
n1=n1';
n2= [];
BB= [];
CC= [];
for I=1:max(size(n1))
    temp1=n1(I)/ratio;
    temp2=round(temp1);
    temp3=abs(temp2-temp1);
    temp4=temp3*Lam2;
    if temp4<Tol
        AA=temp4;
        BB= [BB; I];
        CC= [CC; temp2 I AA];
    end

    n2= [n2; temp3];
end
for I=1:50
end
```

CERTIFICATE OF COMPLETENESS

It is hereby certified that the dissertation submitted by NS Muhammad Adnan Khan, Reg No. **00000205648**, Titled**:** ***A simplified analytical method for wound pressure vessel design*** has been checked/reviewed and its contents are complete in all respects.

Supervisor's Name: **Dr. Hasan Aftab Saeed** Signature: _____

Date: _____